# Cropping Pattern Classification Using Artificial Neural Networks and Evapotranspiration Estimation in the Eastern Mediterranean Region of Turkey

**Omar ALSENJAR[a]** , **Mahmut CETIN[a]** , **Hakan AKSU[b]** , **Mehmet Ali AKGUL[c]** , **Muhammet Said GOLPINAR[a]**

[a]Department of Agricultural Structures and Irrigation, Faculty of Agriculture, Cukurova University, Adana, Turkey
[b]Department of Meteorological Engineering, Ozdemir Bayraktar Faculty of Aeronautics and Astronautics, Samsun University, Samsun, Turkey
[c]The Sixth Regional Directorate of State Hydraulic Works, Adana, Turkey

ABSTRACT

Determining cropping patterns is crucial for quantifying irrigation water requirements at a catchment scale. For this reason, new and innovative technologies such as remote sensing (RS) and artificial neural networks (ANNs) are robust tools for generating the spatiotemporal variation of crops. In line with this, this study aims to classify each crop type using the ANN algorithm and calculate crop evapotranspiration (ETc). This study was conducted in the Akarsu Irrigation District (9495 ha) in the Lower Seyhan Plain in southeastern Turkey in the 2021 hydrological year. Crop types were classified using the ANN algorithm in the Environment for Visualizing Images (ENVI) program based on combined data from Sentinel-2 images with a 10-m resolution and ground truth data collected during the winter and summer seasons. The image analysis results demonstrated that bare soil and citrus made up 3666 ha and 3742 ha respectively in the winter season, while first crop corn (1586 ha) and citrus (4121 ha) were

preponderant in summer. The confusion matrix of the ANN algorithm showed high agreement (wheat 89.76%, onion 91.67%; citrus 97.67% in winter and 98.98% in summer; 100% for lettuce, potato, sesame-2, palm, and watermelon) and medium agreement (fruit 58.33% in winter, 42.86% in summer) with ground truth data in growing seasons. Furthermore, the agreement was more than 80% for the first and second crops (cotton, soybean, peanut, and corn) in the summer season. Annual reference evapotranspiration and ETc were around 1308 mm and 890 mm, respectively. The ETc values for wheat, citrus, first-crop corn, and second-crop soybean were found to be consistent with previous studies of direct evapotranspiration methods conducted in the Cukurova region. Overall, RS and ANNs can be used to classify crop types accurately in the growing season. This study builds upon and expands the application of RS and ANNs in large-scale irrigation schemes.

Keywords: Crop-type classification, Crop evapotranspiration, Sentinel-2, Supervised classification, Remote sensing

## 1. Introduction

Cropping patterns are defined as the areal coverage under different crops at different periods. It also refers to the time and spatial order or succession of crops and/or uncultivated in a specific agricultural area. As pointed out, among others, by Cetin (2020), the types of cultivated plants are subject to change spatiotemporally since market demand and climate conditions are variable in time. However, the determination of crop types in a large-scale irrigation catchment is not an easy task. Crop classification can provide farmers, irrigation water managers, irrigation authorities, engineers of water user associations, etc., with essential and precise information on the crop type by using remotely sensed data coupled with ground truth data. Zheng et al. (2015) indicated that the satellite imagery selection for crop classification is based on, among many other things, image availability, variety level in crop types, and land area extent.

Remote sensing (RS) methods based on optical and/or microwave sensors have become increasingly common in order to extract crop information that explains the vegetation conditions and biophysical crop properties (Yildirim & Asik 2018). RS technology not only provides continuous and large spatial coverage on a large scale (Aksu & Arikan 2017; Oguz 2015) but also provides precision and confidence in the final products. For this reason, RS techniques have been widely applied for drought monitoring (Aksu et al. 2022),

precipitation (P), temperature, water resource, and agricultural monitoring (Kuzay et al. 2022) in large- or small-scale areas. RS also provides availability of information (freely) on crop growth and health status to the farmers (Jayanth et al. 2021). Among other satellites, the Sentinel-2 satellite has thirteen spectral bands with 5-day temporal resolution, which makes it the most popular satellite for vegetation mapping.

A review of the literature shows that the Sentinel-2 has been widely used in precision agriculture for crop monitoring applications (Whyte et al. 2018; Sonobe et al. 2017; Belgiu & Csillik 2018). Five major crop types and non-agriculture areas in Ukraine, Mali, and South Africa and five local locations distributed over the world were classified using the Sentinel-2 and Landsat 8 data (Defourny et al. 2019). They reported that the average accuracy of classification for all areas, with one exception, was higher than 80%. Moreover, Jiang et al. (2020) obtained a mean accuracy of 94% for producing a map using Sentinel-2 satellite imagery for major crop types in three vast sites located in China (each site has between 2 and 3 crops). It must be remembered, however, that classification accuracy is subject to plant species that show changes depending on the climate change phenomenon.

In the Seyhan River basin, climate projections by Columbia University's Center for Climate System Research (CCSR) and the Metrological Research Institute (MRI) of Japan have shown increasing temperature trends (+2.7 °C and +2 °C change by CCSR and MRI, respectively) and decreasing P (159 mm by MRI and 161 mm by CCSR) for the future period up to 2080 (Selek et al. 2016). Increasing temperatures will not only accelerate evapotranspiration rates but also affects plant species. With this in mind, the areal extent of crop types and, hence, estimation of crop evapotranspiration (ETc) is of critical importance. As such, to estimate ETc precisely, crop classification is paramount. Crop data and the development stages of each crop are used to estimate ETc which is determined by multiplying reference evapotranspiration (ETo) by crop coefficient (Kc) according to the crop type and different vegetative stages (Aksu & Arikan 2017; Cetin 2020). The Penman-Monteith (PM) model is one of the best indirect methods for ETc estimation, and has been used commonly in a considerable amount of research in recent years (Santos et al. 2019). In the same context, PM is considered a standard by scientists, irrigators, and the Food and Agriculture Organization because it takes into account all the climatic variables (Santos et al. 2019; Allen et al. 1998).

This study highlights how to determine cropping patterns by using the Artificial Neural Networks (ANNs) algorithm with Sentinel-2 data and ground truth data to better understand and monitor the growth stages of crops and estimate crop biophysical parameters. This study is considered the first attempt to classify cropping patterns in the Akarsu Irrigation District (AID) in the LSP of Turkey. The overall objective of this study is to (1) classify crop types by using the ANN algorithm with the Sentinel-2 satellite images and ground truth data and (2) estimate ETc based on ETo by the PM model using the data of two meteorological stations over the study area.

## 2. Material and Method

The flowchart for ETc calculation, known as a "two-step" procedure, in this study is presented in Figure 1. Figure 1 summarizes the details of the data as well as the methods adopted in detail below.
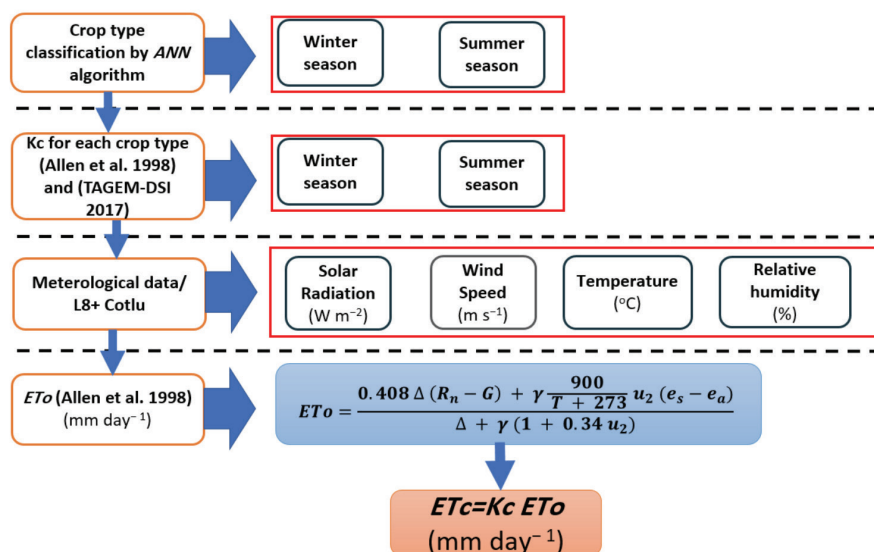


Figure 1- Methodology followed for crop evapotranspiration (ETc) calculation by a "two-step" procedure

*2.1. Study area*

The study area, AID, covers an area of approximately 95 km² (9495 ha). The AID is situated in the LSP and located between 36°57'and 36°51'N latitudes and 35°40' and 35°29'E longitudes, and is noted for its substantially flat terrain (Figure 2). The Mediterranean climate - characterized by hot and dry summers and warm and rainy winters - prevails in the study area. The annual daily average, minimum and maximum air temperatures are 18.9 °C, 9.0 ºC, and 31.0 ºC, respectively. The annual mean P of the Seyhan River basin is around 649.5 mm (Cetin et al. 2020). The hydrological year in Turkey and the AID covers the period between the 1st of October of one year and the 30th of September of the next year. Major crops grown in the AID include cereals, potatoes, onions, and lettuce in the winter season, while summer crops include corn, cotton, soybeans, groundnuts, and watermelons (Ozcan et al. 2003), regardless of whether they are a first or second crop.
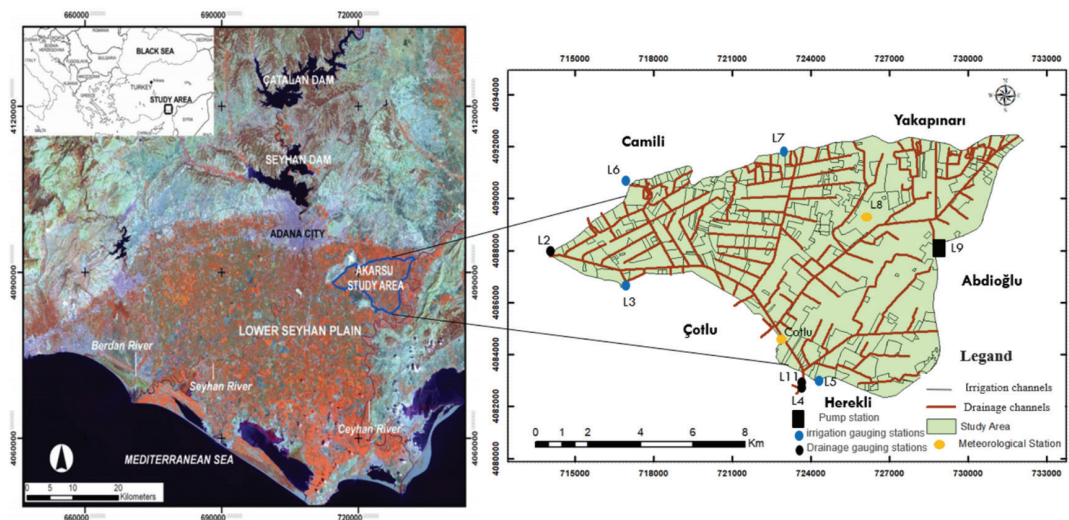


**Figure 2- The Akarsu Irrigation District in the Lower Seyhan Plain, in the Eastern Mediterranean region of Turkey**

*2.2. Crop type processing*

Crop classification results provide crucial data on crop types at the regional scale and thus on cropping patterns. The flowchart, given in Figure 3, presents the required steps to implement the ANN algorithm to classify crop types in the winter and summer seasons using remotely sensed data coupled with ground truth data on the AID. To generate the most accurate insights, we combined data from Sentinel-2 images and ground truth data obtained by surveying different croplands or fields in both the winter and summer seasons. Since splitting the data into two parts (80% for training and 20% for testing) is a generally accepted practice in data science (Mahlayeye et al. 2022) and geospatial modelling (Boken et al. 2004), the same procedure was applied in this research. Moreover, the procedure of the ANN algorithm was followed to detect field boundaries and classify different types of crops. To achieve high degrees of accuracy in the classification process, Normalized Difference Vegetation Index (NDVI), ranging from -1.0 to +1.0, was also determined and included in the study as shown by Rouse et al. (1973).

The NDVI values were calculated as the following by using the Sentinel-2 Satellite Imagery:

$$NDVI= \frac{(NIR_{band8} - Red_{band4})}{(NIR_{band8} + Red_{band4})} \tag{1}$$

where $NIR_{band}$ and $Red_{band}$ are the "*near-infrared*" and "*red*" reflectance, respectively.

Sentinel-2A-2B images, the details of which are given in Table 1, are obtainable at https://scihub.copernicus.eu/dhus/#/home. The crop-type classification was performed in Environment for Visualizing Images (ENVI) software using the "Neural Net Classification" module under "Supervised Classification"; the logistic activation method was used, and three hidden layers were selected. In detail, the input layers are 10 regions in the winter season and 16 regions in the summer, each region presents a crop type as a region of interest (ROI). The links between the input layers and three hidden layers take different weights and are trained depending on the required

output (classified map). To improve classification accuracy, a band is added to the calculated NDVI image as remote sensing data. Furthermore, ground truth data were converted to the ROI format and entered into the ENVI program, along with 5-band (Red, Green, Blue, NIR, and NDVI) images. The Neural Net root mean square (RMS) curve, which was drawn against the iteration value, was extracted separately for both the 2021 winter and 2021 summer classification maps, and the iteration value with the minimum RMS value, as suggested strongly by Boken et al. (2004), was used in the classification. Concordantly, following the steps given in Figure 3, pre-processing of the image data was performed before classification.
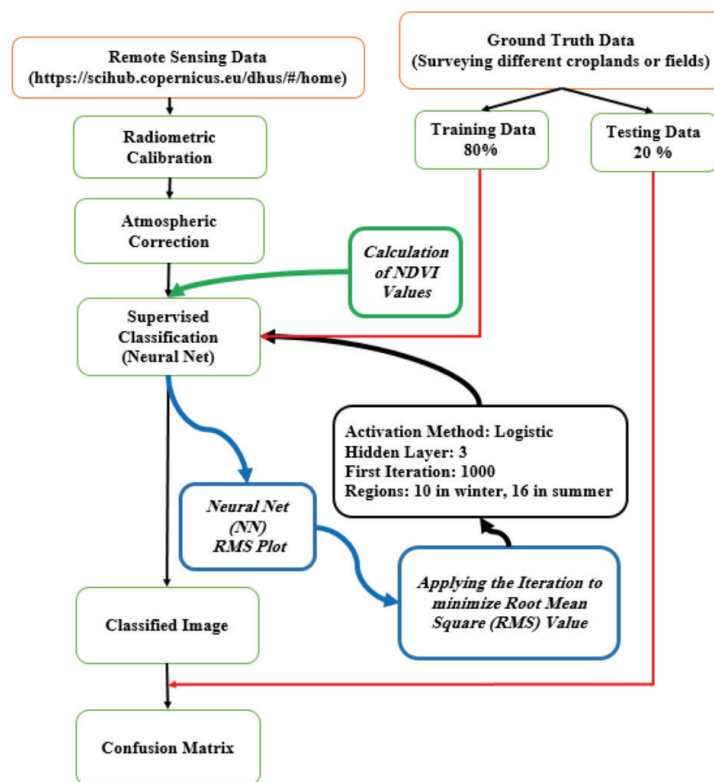


**Figure 3- Methodology followed for ANN procedure by ENVI program using remotely sensed data coupled with ground truth data**

**Table 1- Satellite image names and dates of the images used in the acquisition of summer and winter cropping patterns in the research area**

| Image name | Date |
|---|---|
| S2B_MSIL2A_20200413T082559_N0214_R021_T36SYF_20200413T115830 | 13.04.2020 |
| S2B_MSIL2A_20200702T082609_N0214_R021_T36SYF_20200702T122946 | 02.07.2020 |
| S2A_MSIL1C_20200806T082611_N0209_R021_T36SYF_20200806T100018 | 06.08.2020 |
| S2B_MSIL2A_20210329T082559_N0214_R021_T36SYF_20210329T111602 | 29.03.2021 |
| S2B_MSIL2A_20210627T082559_N0300_R021_T36SYF_20210627T112602 | 27.06.2021 |
| S2A_MSIL2A_20210811T082601_N0301_R021_T36SYF_20210811T114551 | 11.08.2021 |

### 2.3. Crop Evapotranspiration (ETc) Estimation

ETc, as in Equation 2, is calculated by multiplying ETo by Kc according to the crop type and different vegetative stages. This methodology is known as a "two-step" procedure (Steduto 2000).

$$ETc = Kc \; ETo \tag{2}$$

where ETc is crop evapotranspiration, ETo is reference evapotranspiration in the unit of mm day$^{-1}$, and Kc is crop coefficient for a single crop depending on the crop's stage of development. In this study, the standard single Kc value was chosen, as proposed by Allen et al. (1998) and the tables provided by The General Directorate of Agricultural Research And Policies-The State Hydraulic Works (TAGEM-

DSI) (2017) have been used. In addition, Kc values consider the status of the crop at the time of growth stage in different times of growth stages, i.e., initial crop development, mid-season (second and third stages), and late-season, for crops, which are common in the winter and summer seasons in the LSP of Turkey. Allen et al. (1998) modified the PM method to estimate ETo (Equation 3). Equation 3 was developed for short grass; more information, if needed, related to Equation 3 has been provided by Allen et al. (1998).

$$ETo = \frac{0.408\,\Delta\,(R_n - G) + \gamma\frac{900}{T+273}\,u_2\,(e_s - e_a)}{\Delta + \gamma\,(1 + 0.34\,u_2)}$$

(3)

where *ETo* is the reference evapotranspiration (mm day$^{-1}$), $R_n$ is the net radiation at the crop surface (MJ m$^{-2}$day$^{-1}$), *G* is the soil heat flux density (MJ m$^{-2}$day$^{-1}$), *T* is the mean daily air temperature at 2 m height (°C), $u_2$ is the wind speed at 2 m height (m s$^{-1}$), $e_s$ is the saturation vapour pressure (kPa), $e_a$ is the actual vapour pressure (kPa), $e_s$-$e_a$ is the saturation vapour pressure deficit (kPa), *Δ* is the slope of the vapour pressure-temperature curve (kPa°C$^{-1}$), and *γ* the psychrometric constant (kPa°C$^{-1}$).

In this study, climatic variables on hourly and daily time scales were obtained from two automatic meteorological stations, shown in Figure 2, and we applied quality control checks to meteorological data. For this purpose, Cotlu and L8 meteorological stations, as seen in Figure 2, were established and operated in the research area.

# 3. Results and Discussion

## 3.1 Precipitation and reference evapotranspiration (ETo)

Meteorological data observed at the meteorological stations in the study area in the 2021 water year indicated that the climatic conditions of the district and its environs are conducive to agriculture throughout the year. The study area is characterized as hot and dry in summer, and rainy and cool in the winter. Therefore, as seen in Figure 4, ETo ranged between 0.67 mm day$^{-1}$ (minimum value on January 14, 2021) and 8.08 mm day$^{-1}$ (maximum value on July 28, 2021). In addition, Figure 5 shows the temporal variability in monthly ETo values, ranging from 43 mm (all-time low in both December and January) to 189 mm (all-time high in July). The annual cumulative ETo was around 1308 mm for the 2021 hydrological year. As seen in Figure 4, variability in daily P and ETo is more distinctive than in monthly ones. As can be seen from the results, the annual mean ETo and its standard deviation were around 3.59 mm day$^{-1}$ and 1.80 mm day$^{-1}$ ($S^2$=3.24), respectively. A higher variance in daily reference evapotranspiration indicates greater temporal variability in the data (CV≈50%), implying more meteorological stations are needed in the District. The annual total P of the 2021 water year decreased by 183 mm to the annual mean P of the basin (Cetin et al. 2020). Based on the meteorological observations, most of the rainfalls occurred in the winter season, the cumulative P was 382 mm in the winter season of the 2021 water year, whereas rainfall events rarely took place in the summer season.
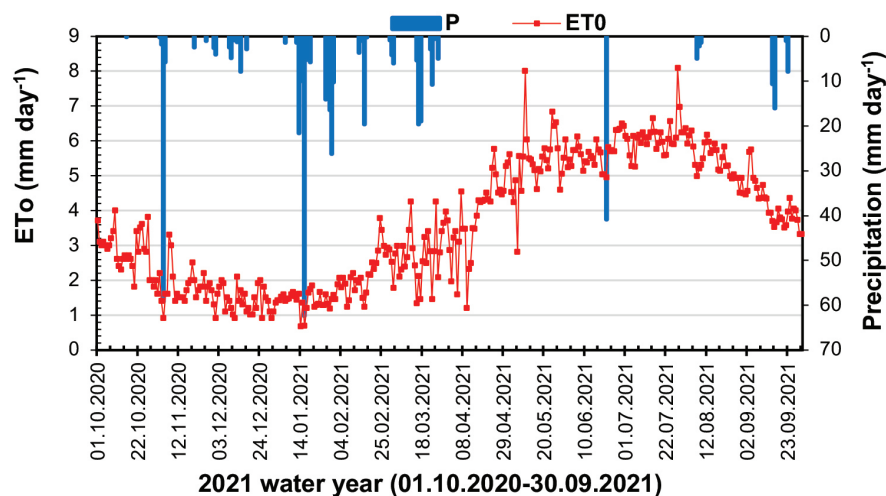


**Figure 4- Temporal variations of precipitation and ETo over the study area in the 2021 water year**
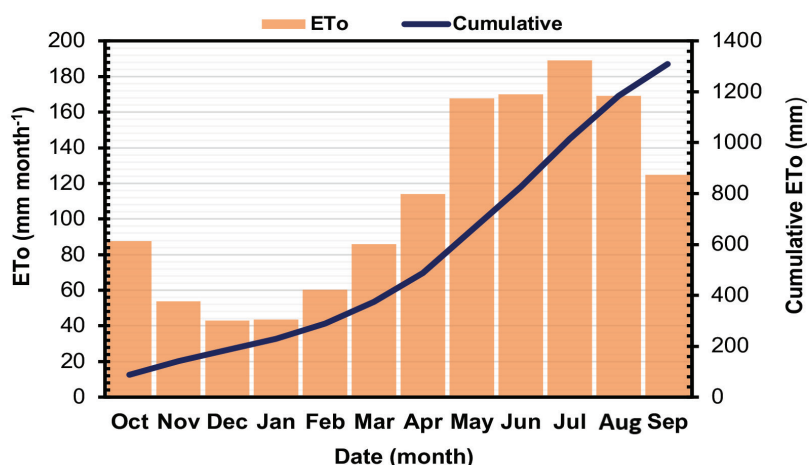
**Figure 5- Monthly ETo values and cumulative reference evapotranspiration during the 2021 hydrologic year**

### 3.2. Crop type classification

Figure 6 shows the results of the crop classification both in the winter and summer seasons. Classification of crop types by ANN algorithm coupled with the ground truth data (for each parcel) resulted in a changing cropping pattern over the study area. A total of 1,316 ground-truth data were used for crop classification in the winter and 1,469 in the summer. Eighty per cent of the dataset was used in training and twenty per cent in testing. Finally, a high classification accuracy (more than 90%), on average for most crops, was obtained over the study area, regardless of the summer or winter season. Mahlayeye et al. (2022) pointed out that cropping patterns are distinguished through their designed spatial arrangement within a field. The cropping pattern results presented in this study (Figure 6) showed parallelism with the cropping pattern examples, i.e., spatial clustering, given in Mahlayeye et al. (2022). For example, as can be seen in Figure 6, citrus-planted areas were dominant in the eastern parts of the study area throughout the year. However, a significant part of the land is empty (bare soil) in winter, and reserves are kept for the first crop in the summer season. On the other hand, corn as the first (Corn-1) and second (Corn-2) crop was the most common crop (18.6%) in the summer season. The pie charts in Figure 7 show the percentage of crop types by summer and winter seasons.
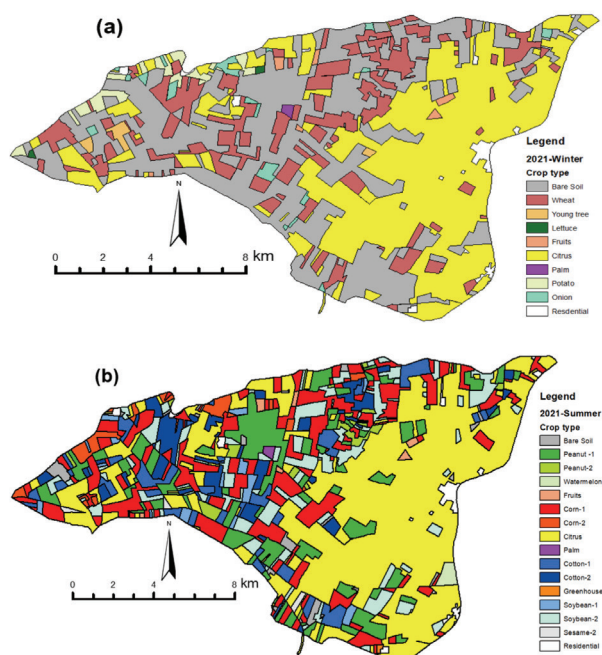


**Figure 6- Crop types distribution over the study area: in winter (a) and in summer (b)**
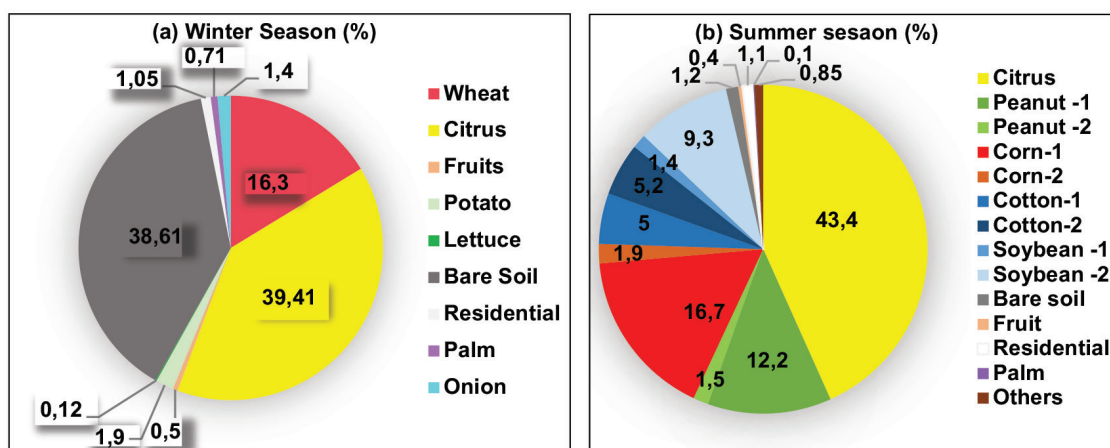
**Figure 7- The percentage of area covered by plants cultivated in the research area in the winter and summer of 2021**

When the ANN algorithm by the ENVI software was applied, a confusion matrix was obtained for the winter and summer seasons (Table 2,3). As seen in Table 2, wheat-grown areas were confused with citrus plantations (3.41%) and bare fields (6.83%) in the winter season while fruit plantations were confused with citrus plantations (33.33%) and bare soil (8.33%). This type of confusion can be explained by the fact that fruit plantations and small citrus trees have the same land characteristics in winter since small citrus seedlings occupy only a very small area of the land. In addition, onion-planted areas were confused with bare soil (8.33%). During the collection of the ground truth data on March 1 to 7, 2021, we observed that wheat and onion crops partially covered the land. For this reason, onion- and wheat-planted fields were faultily classified as bare soil in generated cropping pattern maps (Table 2).

Likewise, a confusion matrix was acquired for the crops grown in the summer season (Table 3). Based on results from Table 3, fruit-planted areas have the highest level of confusion with citrus plantations (42.86%) owing to either their same shape formation or coverage characteristics. Hence, the ANN algorithm in the ENVI software defectively classified fruit trees as citrus plantations. Additionally, Corn-1, Corn-2, Peanut-1, Peanut-2, Soybean-1, Soybean-2, and fruit fields were confused with citrus trees from 0.82% to 42.86% as shown in Table 3. Luckily, Soybean-1 was confused with Soybean-2 (15.38%); this confusion can be explained plainly that the first- and second-crop soybean have the same shape formation (height, width, and leaf development, etc.) at the time of ground truth data acquisition.

**Table 2- Confusion matrix of crop types (%) by ANN classification in the winter season**

| | Class | Bare soil | Wheat | Lettuce | Fruit | Citrus | Palm | Potato | Onion |
|---|---|---|---|---|---|---|---|---|---|
| | | | | | | *Truth* | | | |
| *Predicted* | Bare Soil | 93.68 | 3.02 | 0.00 | 0.00 | 3.30 | 0.00 | 0.00 | 0.00 |
| | Wheat | 6.83 | 89.76 | 0.00 | 0.00 | 3.41 | 0.00 | 0.00 | 0.00 |
| | Lettuce | 0.00 | 0.00 | 100.00 | 0.00 | 0.00 | 0.00 | 0.00 | 0.00 |
| | Fruit | 8.33 | 0.00 | 0.00 | 58.33 | 33.33 | 0.00 | 0.00 | 0.00 |
| | Citrus | 7.33 | 0.00 | 0.00 | 0.00 | 92.67 | 0.00 | 0.00 | 0.00 |
| | Palm | 0.00 | 0.00 | 0.00 | 0.00 | 0.00 | 100.00 | 0.00 | 0.00 |
| | Potato | 0.00 | 0.00 | 0.00 | 0.00 | 0.00 | 0.00 | 100.00 | 0.00 |
| | Onion | 8.33 | 0.00 | 0.00 | 0.00 | 0.00 | 0.00 | 0.00 | 91.67 |

**Table 3- Confusion matrix of crop types (%) by ANN classification in the summer season**

| Predicted \ Class | Truth | | | | | | | | | | | | | |
|---|---|---|---|---|---|---|---|---|---|---|---|---|---|---|
| | Citrus | Corn-2 | Corn-1 | Cotton-1 | Peanut-1 | Soybean-2 | Cotton-2 | Bare Soil | Sesame-2 | Soybean-1 | Peanut-2 | Fruit | Palm | Watermelon |
| Citrus | 98.98 | 0.00 | 0.51 | 0.00 | 0.51 | 0.00 | 0.00 | 0.00 | 0.00 | 0.00 | 0.00 | 0.00 | 0.00 | 0.00 |
| Corn-2 | 3.45 | 86.21 | 6.90 | 0.00 | 0.00 | 0.00 | 0.00 | 0.00 | 0.00 | 0.00 | 0.00 | 3.45 | 0.00 | 0.00 |
| Corn-1 | 5.75 | 0.44 | 85.40 | 1.33 | 2.21 | 3.10 | 0.44 | 0.00 | 0.00 | 0.00 | 0.00 | 1.33 | 0.00 | 0.00 |
| Cotton-1 | 0.00 | 0.00 | 2.70 | 89.19 | 0.00 | 2.70 | 5.41 | 0.00 | 0.00 | 0.00 | 0.00 | 0.00 | 0.00 | 0.00 |
| Peanut-1 | 6.77 | 0.00 | 3.76 | 0.00 | 85.71 | 2.26 | 0.00 | 0.00 | 0.00 | 0.00 | 0.75 | 0.75 | 0.00 | 0.00 |
| Soybean-2 | 0.82 | 0.00 | 4.92 | 0.00 | 0.00 | 90.98 | 1.64 | 0.82 | 0.00 | 0.82 | 0.00 | 0.00 | 0.00 | 0.00 |
| Cotton-2 | 4.05 | 0.00 | 2.70 | 1.35 | 0.00 | 0.00 | 91.89 | 0.00 | 0.00 | 0.00 | 0.00 | 0.00 | 0.00 | 0.00 |
| Bare Soil | 7.14 | 0.00 | 10.71 | 0.00 | 0.00 | 0.00 | 0.00 | 85.71 | 0.00 | 0.00 | 0.00 | 0.00 | 0.00 | 0.00 |
| Sesame-2 | 0.00 | 0.00 | 0.00 | 0.00 | 0.00 | 0.00 | 0.00 | 0.00 | 100.00 | 0.00 | 0.00 | 0.00 | 0.00 | 0.00 |
| Soybean-1 | 3.85 | 0.00 | 0.00 | 0.00 | 0.00 | 15.38 | 0.00 | 0.00 | 0.00 | 80.77 | 0.00 | 0.00 | 0.00 | 0.00 |
| Peanut-2 | 5.71 | 0.00 | 8.57 | 0.00 | 0.00 | 2.86 | 5.71 | 0.00 | 0.00 | 0.00 | 77.14 | 0.00 | 0.00 | 0.00 |
| Fruit | 42.86 | 0.00 | 0.00 | 0.00 | 0.00 | 0.00 | 0.00 | 0.00 | 0.00 | 0.00 | 0.00 | 42.86 | 14.29 | 0.00 |
| Palm | 0.00 | 0.00 | 0.00 | 0.00 | 0.00 | 0.00 | 0.00 | 0.00 | 0.00 | 0.00 | 0.00 | 0.00 | 100.00 | 0.00 |
| Watermelon | 0.00 | 0.00 | 0.00 | 0.00 | 0.00 | 0.00 | 0.00 | 0.00 | 0.00 | 0.00 | 0.00 | 0.00 | 0.00 | 100.00 |

## 3.3. Temporal Variability in Crop Evapotranspiration

The values of ETc were estimated based on the ETo and Kc for crop types that were classified using the ANN algorithm. Table 4 shows the monthly ETc for each crop type. In addition, Figure 8 shows the variation of monthly ETc over the AID; the yearly ETc was about 890 mm for the 2021 water year. Based on the results of Table 4, it is of great importance to highlight that the highest and the lowest calculated ETc values were for Cotton-1 and onion, respectively. In this regard, the ETc on a yearly basis was highest for cotton followed by citrus, and corn. Research results conducted by Boken et al. (2004) noted that the irrigation depth for cotton was greater than that of corn, supporting our own findings. On the other hand, in the winter season, wheat and potato are the highest water-demanding crops in the AID. At the same time, Cotton-1, Corn-1 and Peanut-1 are highly water-intensive crops when compared with other crops in the summer season. For the whole year, ETc for deciduous fruit trees such as apple, pomegranate, peach, plum, etc., and evergreen trees such as citrus (lemon, mandarin, orange, grapefruit, etc.) was around 1008 mm and 889 mm, respectively. As shown in Table 4, the values of ETc for second crops like Corn-2, Cotton-2, Soybean-2, and Peanut-2 are lower than the first crop ETc. The likely reason may be that Kc values, which vary by the crop development stages, and sowing dates, hence, the length of the growing period, and harvesting periods for second crop types, are slightly smaller than those of the first crops. In this context, several studies have been done to estimate ETc in the Cukurova region in which our study area was located. Table 5 shows measured ETa by direct methods, ETa using the Soil and Water Assessment Tool (SWAT) model obtained from the existing literature, and the calculated ETc in the 2021 water year. As seen in Table 5, one of the studies estimated the actual evapotranspiration (ETa) for Soybean-2 in 2009 by the lysimeter and Bowen Ratio-Energy Balance (BREB). The seasonal cumulative ETa for Soybean-2 by the lysimeter was 354 mm in the period of the growing season (from 25.06.2009 to 06.10.2009), whereas BREB was 405 mm (Unlu et al. 2010) in the same period. As understood clearly from these two figures, the ratio of ETa by BREB to ETa by lysimeter is 1.14, indicating that lysimeter estimates are equal to 87% of BREB estimates in the same period and there exists inherited variability in ET estimation methods. In turn, the difference in ETc value for Soybean-2 (ETc=562.1 mm) in the 2021 water year in our study and ETa values in 2009 for Soybean-2 (ETa=354 mm by lysimeter and ETa=405 mm by BREB) may be explained by the inherent spatio-temporal variability in climate data and Kc selection in the ETc method. Another study by Nur (2019) was conducted to determine Corn-1 (maize) evapotranspiration in the Cukurova region, between 28.04.2012 and 02.09.2012 by using the lysimeter method and water budget method under the Cukurova conditions. The seasonal ETa for Corn-1 was determined as 618.2 mm and 488.8 mm by using the weighted lysimeter method and water budget method, respectively. In the same context, the ETc value

(841.4 mm) obtained in this study for Corn-1 in the 2021 water year was higher than the ETc values by lysimeter and water budget methods (618.2 mm and 488.8 mm, respectively) for Corn-1 in the 2012 water year. Based on the results, it may be concluded that the difference between the seasonal ETa values for first crop corn (Corn-1) obtained from the lysimeter and the water budget method is almost 26%, but a 36% difference between ETa by lysimeter and ETc by Kc in this study. It should be kept in mind that, let alone the stochastic behaviour in the ETc, the ETc values in this study are subject to climatic variables observed in the 2021 water year and regional Kc values acquired from TAGEM-DSI (2017). Therefore, a 36% difference might be quite reasonable. Another possible reason for the difference could be the values of Kc in the ETc method because Kc values are related to development growth stages. Put another way, ETc calculations do not consider the stressed conditions, but direct methods for ETa estimation. A study by Koc & Kanber (2020) estimated wheat evapotranspiration as 708 mm by using the water balance method under irrigated conditions in the Cukurova region in the 2004 water year. The Kc values for wheat may be the reason behind the difference in values of the ETc method and a possible reason to explain the difference between the ETc method (488.9 mm in this study) and the water balance method for wheat in the 2021 and 2004 water years. Akpolat (2011) estimated the ETa of wheat under rainfed conditions, by using BREB and lysimeter methods in the Cukurova region in the 2010 water year. The seasonal ETa of rainfed wheat (between 19.11.2009 and 25.05.2010) was found to be 321 mm and 376 mm for the BREB and lysimeter methods, respectively. In the 2010 hydrological year, wheat was based only on rainfalls and there was no irrigation. Therefore, the actual ETa for wheat in 2010 was less than the ETc of 488.9 mm in this study in the 2021 water year. Although ETc is crop water requirement, ETa is the water consumed actually by the crop. Hence, ETa is subject to stressed conditions and the availability of water during the growing season. For example, a study for determining the ETa of wheat was performed by Yildiz (2019) under rainfed conditions in the Cukurova region between the 2014 and 2015 growing seasons. Seasonal rainfed wheat evapotranspiration was measured as 368 mm by the lysimeter method, 312 mm by the eddy covariance (EC) method, and 335 mm by using the water budget method. The rainfed wheat evapotranspiration value (2014-2015) was ≈33% lower than the wheat ETc method (488.9 mm) in the 2021 hydrological year. In other words, seasonal wheat evapotranspiration grown under natural rainfall conditions is less than the ETc method which takes into consideration rainfalls and irrigation together. Unlu et al. (2011) estimated cotton evapotranspiration by using a water balance model for drip-irrigated full (100%) and deficit (70% and 50%) irrigation from 2005 to 2008 in the Cukurova Region. Cotton evapotranspiration varied between 477 mm and 671 mm in full irrigation and from 376 mm to 398 mm under severe water-stressed conditions. Climate data in the 2021 water year and Kc values in the ETc method could be a reason for the difference between the ETc method and the water balance model for full irrigation treatment results by Unlu et al. (2011). For citrus, Unlu et al. (2014) estimated the ETa of grapefruit trees or a 'Rio Red' grapefruit (Citrus paradisi Macfad. 'Rio Red') orchard through three different irrigation regimes in the Mediterranean environment (in Adana, Turkey) using three methods of EC, BREB, and the water balance method in 2011 and 2012. Their results showed that the annual ET of grapefruit (for full irrigation) was measured as 810.5 mm and 892.9 mm (water balance) for 2011 and 2012, respectively. Moreover, annual grapefruit ET was measured as 716.9 mm and 640.4 mm for the BREB method and EC method, respectively. As seen in Table 4, citrus evapotranspiration values (888.8 mm) are slightly in agreement with yearly grapefruit ETa values obtained by Unlu et al. (2014). On the other hand, Golpinar (2017) estimated the water budget elements, including the potential and ETa, in the AID by using the SWAT from 2009 to 2014. Based on the results, actual ETa values generated by the SWAT model at the catchment level varied from 671.4 mm to 744.7 mm (Golpinar 2017). The cumulative ETc value given in Figure 8, i.e., annual ETc at the irrigation district, in the 2021 water year was higher than the values of ETa between 2009 and 2014 for the same study area (AID). As seen in Figure 8, the monthly ETc values are less than 35 mm per month from November to February. However, it reaches its peak value as ETc=151.3 mm in July, indicating that July is the peak irrigation season in the region. These changes in the value of ETc may be to the result of inherent temporal variability in the climate data from year to year and/or spatial variation in cropping patterns over the years. For example, the difference between the monthly average temperatures observed in 2021 and the monthly average temperatures observed in previous years varied between 1.0-4.4 °C, indicating that monthly temperatures are higher in 2021 than in the previous years. On the other hand, the relative humidity increased at a rate of 6%. Furthermore, Cetin et al. (2020) pointed out that the annual total P (476.6 mm) of 2021 water year decreased by 183 mm (almost 28% less than normal) compared to the annual mean P of the basin. Despite all this, it might be possible that the SWAT model could underestimate or overestimate the ET values based on the ETo estimation method selected.

**Table 4- Monthly and yearly ETc values (mm) for the crop types during the growing seasons (2020-2021)**

| | *Oct* | *Nov* | *Dec* | *Jan* | *Feb* | *Mar* | *Apr* | *May* | *Jun* | *Jul* | *Aug* | *Sep* | *Total* |
|---|---|---|---|---|---|---|---|---|---|---|---|---|---|
| Wheat | - | 24.3 | 35.6 | 44.5 | 69.4 | 98.6 | 111.4 | 91.2 | 13.9 | - | - | - | 488.9 |
| Citrus | 61.4 | 37.7 | 30.1 | 32.7 | 45.2 | 60.0 | 79.8 | 117.5 | 110.6 | 122.9 | 109.9 | 81.1 | 888.8 |
| Corn-1 | - | - | - | - | - | 52.0 | 102.9 | 196.0 | 204.1 | 180.4 | 91.6 | 14.5 | 841.4 |
| Corn-2 | 66.6 | - | - | - | - | - | - | - | 33.4 | 131.3 | 180.4 | 144.2 | 555.9 |
| Cotton-1 | 42.6 | - | - | - | - | 30.2 | 72.2 | 163.0 | 204.1 | 226.9 | 197.9 | 118.9 | 1055.9 |
| Cotton-2 | 76.7 | - | - | - | - | - | - | - | 29.9 | 129.8 | 193.1 | 149.7 | 579.2 |
| Watermelon | - | - | - | - | - | - | 64.0 | 160.3 | 187.1 | 188.9 | - | - | 600.2 |
| Fruit (pomegranate, apple, peach, plum, etc ) | 71.1 | 38.8 | 27.1 | 8.7 | 12.1 | 60.0 | 86.5 | 141.7 | 146.3 | 162.6 | 145.4 | 107.3 | 1007.5 |
| Onion | 43.9 | 32.5 | 40.3 | 45.8 | 58.5 | 40.6 | - | - | - | - | - | - | 261.5 |
| Potato | - | - | 23.6 | 38.9 | 69.4 | 98.6 | 98.1 | - | - | - | - | - | 328.6 |
| Peanut-1 (groundnut-1) | - | - | - | - | - | - | 42.6 | 129.0 | 188.5 | 217.5 | 148.6 | 28.9 | 755.1 |
| Peanut-2 (groundnut-2) | 60.5 | - | - | - | - | - | - | - | 57.3 | 129.4 | 155.5 | 118.5 | 521.3 |
| Soybean-1 | - | - | - | - | - | - | 52.6 | 143.9 | 195.6 | 184.7 | 66.0 | - | 642.9 |
| Soybean-2 | 58.9 | - | - | - | - | - | - | - | 45.8 | 133.8 | 186.0 | 137.5 | 562.1 |
| Sesame-2 | - | - | - | - | - | - | - | - | 115.7 | 199.7 | 185.9 | 88.7 | 590.1 |
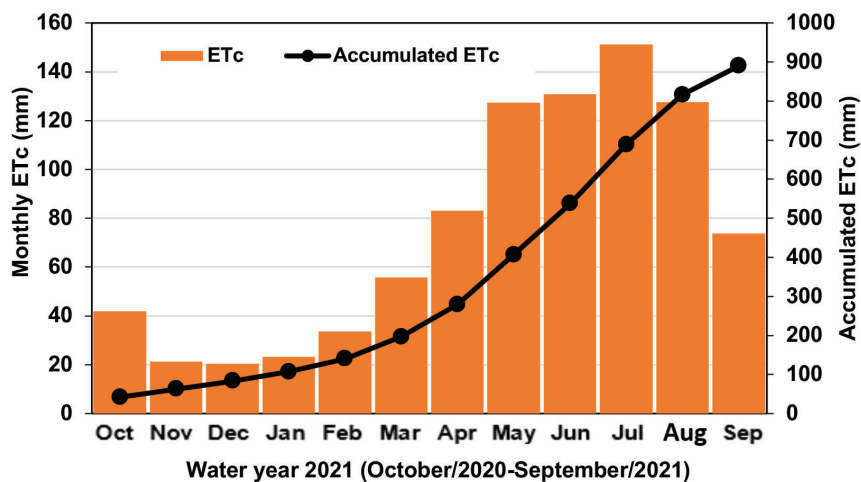


**Figure 8- Monthly ETc values and cumulative ETc during the 2021 water year**

**Table 5- Measured ETa by direct methods, estimated ETa using the SWAT model from the existing literature, and calculated ETc in 2021 water year (mm)**

| Crop type and the whole study area | Years | Measured ETa in the Cukurova region | | | | Estimated ETa | Calculated ETc in 2021 |
|---|---|---|---|---|---|---|---|
| | | Lysimeter | Bowen ratio-energy balance (BREB) | Water budget method | Eddy Covariance (EC) | SWAT | |
| Wheat | 2004 | | | 708.0 Koc & Kanber (2020) | | | 488.9 |
| | 2010 | 376.0 Akpolat (2011) | 321.0 | | | | |
| | 2015 | 368.0 Yildiz (2019) | | 335.0 | 312.0 | | |
| Citrus | 2011 | | 716.9 Unlu et al. (2014) | 810.5 | 640.4 | | 888.8 |
| | 2012 | | | 892.9 Unlu et al. (2014) | | | |
| Corn-1 | 2012 | 618.2 Nur (2019) | | 488.8 | | | 841.4 |
| Cotton-1 for full irrigation | 2005 | | | 671.0 | | | 1055.9 |
| | 2006 | | | 477.0 | | | |
| | 2007 | | | 587.0 | | | |
| | 2008 | | | 601.0 Unlu et al. (2011) | | | |
| Soybean-2 | 2009 | 354.0 Unlu et al. (2010) | 405.0 | | | | 562.1 |
| Study area | 2009 | Golpinar (2017) | | | | 744.7 | 890.0 |
| | 2010 | | | | | 671.4 | |
| | 2011 | | | | | 713.2 | |
| | 2012 | | | | | 670.9 | |
| | 2013 | | | | | 730.0 | |
| | 2014 | | | | | 730.2 | |

## 4. Conclusions

This study applied up-to-date technologies for remote sensing and ANNs jointly to classify crop types by using the Sentinel-2A-2B and ground truth data obtained by field campaigns conducted in the study area in the 2021 hydrological year. In addition, daily ETc by the "two-step" procedure and ETo using the PM model were estimated. Based on crop type classification results and the confusion matrix by the ANN model, the use of Sentinel-2A-2B showed high compatibility with ground truth data. Validation results showed that the estimation accuracy was 100% for lettuce, watermelon, palm, and sesame-2, more than 93% for citrus in both winter and summer seasons, and over 80% for other crops-with the exception of fruit trees. In addition, the discrimination capability of the ANN algorithm for citrus and fruit trees did not achieve a high degree of accuracy in the winter and summer seasons when compared with other crops. The ANN approach helped us to generate sufficiently accurate classified crop distribution maps over large irrigation catchments. In turn, citrus plantations were preponderant in the winter and summer seasons of the 2021 water year with coverages of 39.4% and 43.4%, respectively. Bare soils, i.e., fallow areas, made up 38.61% of the study area in the winter, while first-crop corn (Corn-1) constituted nearly 17% of the study area in the summer. The annual total of ETc and ETo was around 890 mm and 1308 mm in the 2021 water year, respectively. ETc values (Soybean-2, Corn-1, wheat, and citrus) are (to some extent) compatible with previous studies in the literature in the same study area. Essentially, inconsistencies among ETa and ETc values obtained by different methods have been attributed to the inherited spatio-temporal variability in the meteorological data, climate change phenomena, and spatial variations in cropping

patterns over the study area, etc. Moreover, research findings led us to conclude that the use of remote sensing data in cropping pattern determination is promising for providing information frequently and freely with high spatial resolution. RS images and ANNs could be confidently used to classify crop types accurately in different growth stages throughout the growing seasons. As freshwater resources are very limited in the changing world, particularly in Mediterranean countries, disagreements often occur on how to allocate them to water-demanding sectors. For this reason, the proposed method, simple but effectively applicable, for classifying crop types and determining ETc may be a pragmatic remedy to assist water authorities in apportioning irrigation water among both irrigation schemes and, if needed, farmers optimally and equitably in a realistic manner. Furthermore, water user associations, water authorities, and others may adapt the methodology followed in this study to other large-irrigation schemes where cropping patterns are difficult to obtain.

## References

Akpolat A (2011). Mikrometeorolojik ve Lizimetre Yöntemleriyle Belirlenen Buğday Bitki Su Tüketimlerinin Karşılaştırılması. Yüksek Lisans Tezi. Çukurova Üniversitesi Fen Bilimleri Enstitüsü Tarımsal Yapılar ve Sulama Anabilim Dalı, Türkiye. (In Turkish) http://libratez.cu.edu.tr/tezler/8692.pdf

Aksu H & Arikan A (2017). Satellite-based estimation of actual evapotranspiration in the Buyuk Menders Bain, Turkey. *Hydrology Research* 48(2):559-570. doi.org/10.2166/nh.2016.226

Aksu H, Cavus Y, Aksoy H, Akgul M A, Turker S & Eris E (2022). Spatiotemporal analysis of drought by CHIRPS precipitation estimates. *Theor Appl Climatol* 148: 517-529. doi.org/10.1007/s00704-022-03960-6

Allen R G, Pereira L S, Raes D & Smith M (1998). Crop evapotranspiration - guidelines for computing crop water requirements. FAO irrigation and drainage paper 56. *FAO, Rome* 300(9): D05109.

Belgiu M & Csillik O (2018). Remote Sensing of Environment Sentinel-2 cropland mapping using pixel-based and object-based time-weighted dynamic time warping analysis. *Remote Sensing of Environment* 204: 509-523.

Boken V K, Hoogenboom G, Hook J E, Thomas D L, Guerra L C & Harrison K A (2004). Agricultural water use estimation using geospatial modeling and a geographic information system. *Agricultural Water Management* 67(3): 185-199.

Cetin M (2020). Agricultural Water Use. In: Harmancioglu N B, Altinbilek D (eds.), Water Resources of Turkey, World Water Resources, Vol. 2, *Springer Nature Switzerland.* pp. 257-302. doi.org/10.1007/978-3-030-11729-0_9

Cetin M, Kaman H, Kirda C & Sesveren S (2020). Analysis of irrigation performance in water resources planning and management: A case study. *Fresenius Environmental Bulletin (FEB)* 29(05): 3409-3414.

Defourny P, Bontemps S, Bellemans N, Cara C, Dedieu G, Guzzonato E, Hagolle O, Inglada J, Nicola L & Rabaute T (2019). Near real-time agriculture monitoring at national scale at parcel resolution: Performance assessment of the Sen2-Agri automated system in various cropping systems around the world. *Remote Sensing of Environ* 221: 551-568.

Golpınar M S (2017). Yüzey Akişlarin Swat Modeli ile Belirlenmesi: Akarsu Sulama Birliği Sahasi Örneği. Yüksek Lisans Tezi. Çukurova Üniversitesi Fen Bilimleri Enstitüsü Tarımsal Yapılar ve Sulama Anabilim Dalı, Türkiye. (In Turkish)

Jayanth J, Aravind R & Amulya C M (2021). Classification of crops and crop rotation using remote sensing and GIS-Based approach: A case study of Doddakawalande Hobli, Nanjangudu Taluk. *Journal of the Indian Society of Remote Sensing* 50: 197-215. doi.org/10.1007/s12524-020-01296-0

Jiang Y, Lu Z, Li S, Lei Y, Chu Q, Yin X & Chen F (2020). Large-scale and high-resolution crop mapping in China using sentinel-2 satellite imagery. *Agriculture* 10(10): 433. doi.org/10.3390/agriculture10100433

Koc D L & Kanber R (2020). Determination of evapotranspiration for wheat by Using Bowen Ratio Energy Balance Method. *KSU J Agric Nat* 23(2): 544-553. DOI: 10.18016/ksutarimdoga.vi.597980

Kuzay M, Tuna M & Tombul M (2022). Determining the relationship of evapotranspiration with precipitation and temperature over Turkey. *Journal of Agricultural Sciences* 28(3): 525-534. doi.org/10.15832/ankutbd.952845

Mahlayeye M, Darvishzadeh R & Nelson A (2022). Cropping Patterns of Annual Crops: A Remote Sensing Review. *Remote Sens* 14(10): 2404. doi.org/10.3390/rs14102404

Nur A (2019). Çukurova Koşullarında Lizimetere Yöntemiyle Mısır Bitki Su Tüketiminin ve Bitki Katsayılarının Belirlenmesi. Yüksek Lisans Tezi. Çukurova Üniversitesi Fen Bilimleri Enstitüsü Tarımsal Yapılar ve Sulama Anabilim Dalı, Türkiye. (In Turkish)

Oguz H (2015). A software tool for retrieving land surface temperature from ASTER imagery. *Journal of Agricultural Sciences* 21(4): 471-482. doi.org/10.1501/Tarimbil_0000001350

Ozcan H, Cetin M & Diker K (2003). Monitoring and Assessment of Land Use Status by Gis. *Environmental Monitoring and Assessment* 87(1): 33-45.

Rouse J, Haas R H, Deering D, Sehell J A & Harlan J (1973). Monitoring the vernal advancement and retrogradation (green wave effect) of natural vegetation. Final Rep. *Remote Sensing Center* 1-112.

Santos L, Da C, Cruz G H T, Capuchinho F F, José J V & Dos Reis E F (2019). Assessment of empirical methods for estimation of reference evapotranspiration in the Brazilian Savannah. *Australian Journal of Crop Science* 13(7): 1094-1104. doi.org/10.21475/ajcs.19.13.07

Selek B , Yazici D D , Aksu H & Özdemir A D (2016). Seyhan Dam, Turkey, and Climate Change Adaptation Strategies, In Increasing Resilience to Climate Variability and Change, *Springer Singapore,* pp. 205-231.

Sonobe R, Yamaya Y, Tani H, Wang X, Kobayashi N & Mochizuki K (2017). Assessing the suitability of data from Sentinel-1A and 2A for crop classification. *GIScience & Remote Sensing* 54(6): 918-938. doi.org/10.1080/15481603.2017.1351149

Steduto P (2000). Plant nutrient management under pressurized irrigation systems in the Mediterranean Region: crop water requirements. In: Ryan J (ed) Plant nutrient management under pressurized irrigation systems in the Mediterranean Region. Proceedings of the International Fertigation Workshop organized by the World Phosphate Institute (IMPHOS), 25-27 April 1999. ICARDA, Aleppo. pp. 400.

TAGEM-DSI (2017). Plant Water Consumption of Irrigated Plants in Turkiye. The Republic of Türkiye, Ministry of Agriculture and Forestry, General Directorates of Agricultural Research and Policies (TAGEM) and State Hydraulic Works (DSI), Published by TAGEM, Ankara, Turkiye. pp. 590.

Unlu M, Kanber R & Kapur B (2010). Comparison of soybean evapotranspirations measured by weighing lysimeter and Bowen ratio-energy balance methods. *African Journal of Biotechnology* 9(30): 4700-4713.

Unlu M, Kanber R, Koc D L, Ozekici B & Kekec U (2014). Irrigation scheduling of grapefruit trees in a Mediterranean environment throughout evaluation of plant water status and evapotranspiration. *Turkish Journal of Agriculture and Forestry* 38(6): 908-915. doi.org/10.3906/tar-1403-58

Unlu M, Kanber R, Koc D L, Tekin S & Kapur B (2011). Effects of deficit irrigation on the yield and yield components of drip irrigated cotton in a Mediterranean environment. *Agricultural Water Management* 98(4): 597-605. doi.org/10.1016/j.agwat.2010.10.020

Whyte A, Ferentinos K P & Petropoulos G P (2018). A new synergistic approach for monitoring wetlands using Sentinels -1 and 2 data with object-based machine learning algorithms. *Environmental Modelling & Software* 104: 40-54.

Yildirim T & Asik S (2018). Index-based assessment of agricultural drought using remote sensing in the semi-arid region of western Turkey. *Journal of Agricultural Sciences* 24(4): 510-516. doi.org/10.15832/ankutbd.337136

Yildiz A M (2019). Çukurova Koşullarında Lizimetre, Eddy Kovaryans ve Su Bütçesi Yöntemleri ile Belirlenen Buğday Bitki Su Tüketimlerinin Karşılaştırılması. Yüksek Lisans Tezi. Çukurova Üniversitesi Fen Bilimleri Enstitüsü Tarımsal Yapılar ve Sulama Anabilim Dalı, Türkiye. (In Turkish)

Zheng B, Myint S W, Thenkabail P S & Aggarwal R M (2015). A support vector machine to identify irrigated crop types using time-series Landsat NDVI data. *International Journal of Applied Earth Observation and Geoinformation* 34: 103-112.